Polarization in p-p elastic scattering at large four-momentum transfers*

G. W. Bryant, M. Corcoran, R. R. Crittenden, S. W. Gray, R. M. Heinz, H. A. Neal,[†] and D. R. Rust

Department of Physics, Indiana University, Bloomington, Indiana 47401

(Received 16 June 1975)

New results are presented from the continuation of an experiment designed to study the polarization in elastic p-p scattering at large four-momentum transfers. A high-intensity unpolarized proton beam of momentum 12.3 GeV/c was incident on a propanediol polarized proton target and both final-state protons were detected and momentum-analyzed in multiwire proportional chamber spectrometers. The measurements spanned the t range $1.5 < |t| < 6.2$ (GeV/c)^2. The results are discussed in the framework of optical, exchange, and parton models.

In this article the final 12.3-GeV/c results are presented from an experiment conducted at the Argonne ZGS accelerator to study the polarization in p-p elastic scattering at large four-momentum transfers. Data from earlier runs and a detailed discussion of the apparatus can be found in Refs. 1, 2, and 3. The experimental technique will be briefly reviewed below and results will be discussed in terms of optical, exchange, and parton models. It will be argued in the following that the feasibility of making differential cross section and polarization measurements in p-p elastic scattering out to very large $|t|$ values provides a unique opportunity to extract information regarding nucleon structure.

The experimental layout is shown in Fig. 1. A high-intensity unpolarized proton beam $(1-7 \times 10^9$ protons per burst) was incident on a propanediol polarized proton target, and the resulting elastically scattered protons were detected and momentum-analyzed in two multiwire proportional chamber spectrometers. Each spectrometer consisted of two sets of four proportional chambers and two trigger counters; one set was located upstream and the other set was located downstream of an analyzing magnet which bent the elastically scattered protons through an angle of approximately 3°. The spectrometers permitted the momentum of the final-state protons to be determined with a resolution of ± 6%, the opening angle to be measured with a resolution of ±4 mrad, and the relative time of flight between the downstream fast and slow proton counters to be determined with a resolution of ±0.7 nsec. These measurements provided sufficient constraints to make the elastic peak predominant in all cases. Examples showing the effect of cuts on the time of flight, the opening angle, and the fast-proton momentum distribution are shown in Refs. 1 and 2. A comparison of distributions for corresponding propanediol and carbon dummy target runs reveals that the quasielastic contamination is small at all points studied.

The flux incident on the polarized target was monitored by two water Cherenkov counters placed in the beam to shadow the target sample, by a counter telescope which viewed scatters from a piece of appropriately sized plastic placed in the incident beam, and by telescopes which detected large-angle scatters from the polarized target. Integrating wire proportional chambers were employed to monitor the position of the incident beam on a burst-to-burst basis. Care was taken to ensure the stability of the beam centroid on the polarized target. With the beam so constrained, the various relative flux monitors were found to be internally consistent to a high degree. To minimize the effects of instrumental biases the target spin was reversed frequently. A typical data point results from approximately 16 target spin reversals. The residual systematic errors are estimated to be small compared to the statistical uncertainties.

The polarized target material utilized in the new measurements was propanediol, and with the new ZGS cryostat PPTV target polarizations of approximately 80% were attained. In our earlier measurements the cryostat employed permitted polarizations of only $\approx 38\%$, and this represents the principal technical difference in the two sets of measurements.

A PDP-15 on-line computing system was employed to record the data from the proportional chambers, counter latches, time-of-flight units, scalers, and the polarized target NMR system and to monitor all critical aspects of the experiment.

The data from the earlier run reported in Ref. 3 were found to be in statistical agreement with data from the present set of measurements, and they have been combined for presentation in Fig. 2 and Table I. The errors shown are statistical only. There exists an additional ±8% normalization uncertainty. Also shown in Fig. 2 are the 10-GeV/c results of Borghini et $al.$[4] The salient
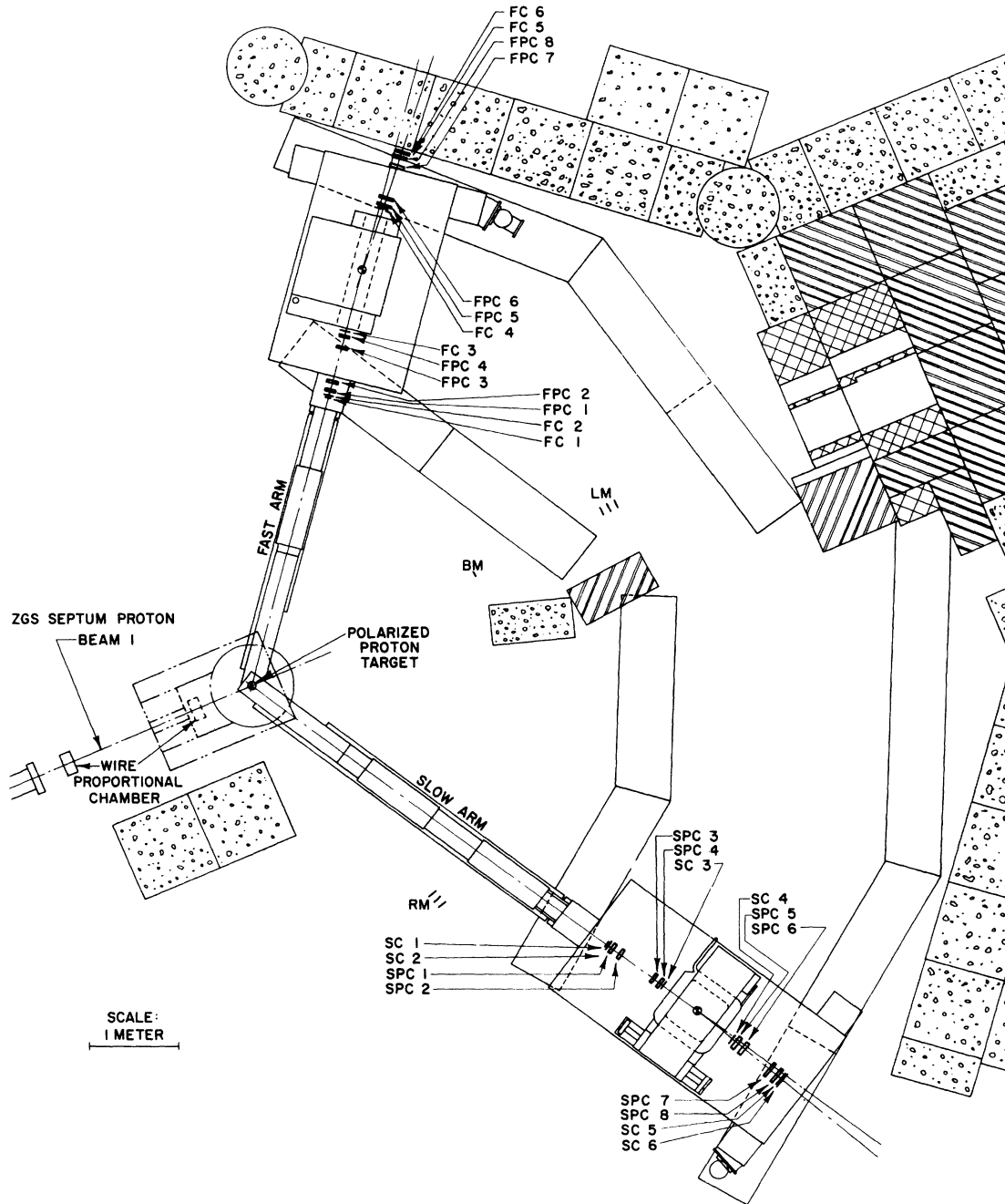
FIG. 1. The experimental layout. Elements labeled $SC1, \ldots, SC6$ and $FC1, \ldots, FC6$ are scintillation counters. Elements labeled $SPC1, \ldots, SPC8$ and $FPC1, \ldots, FPC8$ are multiwire proportional chambers. A magnet capable of bending elastically scattered protons through an angle $> 3°$ is present in each arm (between elements $SC3$ and $SC4$ and between elements $FC3$ and $FC4$). The angular position of each arm is remotely variable. BM, LM, and RM are beam monitors.
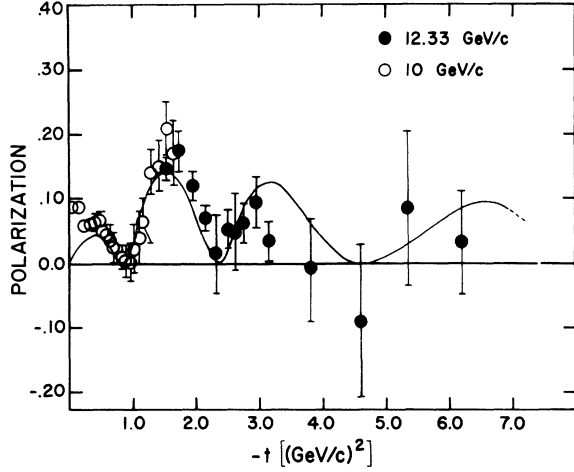
FIG. 2. Polarization in p-p elastic scattering. The solid circles represent data at 12.3 GeV/c from the present experiment. The open circles represent data from Ref. 4 at 10.0 GeV/c. The curve shown represents a fit to the data obtained with the Chu-Hendry optical model (Ref. 7).

features of the data are the relative maxima at $|t| \cong 0.3$ and 1.8 $(GeV/c)^2$ and the double zeros at $|t| \cong 0.7$ and 2.3 $(GeV/c)^2$. As will be argued below, the existence of these double zeros may have substantial importance in determining the amplitude structure.

For the discussion which follows it is convenient to utilize the helicity amplitudes defined by Goldberger et $al.$,[5]

$$\varphi_1 = \langle + + | \varphi | + + \rangle,$$
$$\varphi_2 = \langle + + | \varphi | - - \rangle,$$
$$\varphi_3 = \langle + - | \varphi | + - \rangle, \qquad (1)$$
$$\varphi_4 = \langle + - | \varphi | - + \rangle,$$
$$\varphi_5 = \langle + + | \varphi | + - \rangle.$$

TABLE I. Polarization in p-p elastic scattering at 12.3 GeV/c.

$\theta_{c.m.}$ (deg)	$|t|$ $[(GeV/c)^2]$	P	ΔP
31.0	1.531	0.147	0.020
33.0	1.730	0.175	0.032
35.0	1.939	0.119	0.023
37.0	2.159	0.071	0.020
38.5	2.331	0.015	0.062
40.0	2.508	0.052	0.029
41.0	2.630	0.048	0.060
42.0	2.754	0.062	0.028
43.5	2.945	0.094	0.038
45.0	3.140	0.034	0.031
50.0	3.830	−0.007	0.083
55.0	4.572	−0.092	0.116
60.0	5.361	0.086	0.117
65.0	6.191	-0.033	0.080

The polarization parameter is given by the following relation:

$$P = - \text{Im}[(\varphi_1 + \varphi_2 + \varphi_3 - \varphi_4)\varphi_5^*] \Big/ \frac{d\sigma}{d\Omega}, \qquad (2)$$

where $d\sigma/d\Omega$ is the elastic p-p differential cross section.

The result of various attempts to fit p-p polarization data in the Regge model has been recently reviewed by Hendry and Abshire.[6] To obtain the observed structure in the polarization they note that the condition of exchange degeneracy must be sacrificed and that substantial structure must be introduced in the residue functions. Reasonable fits to the data can be obtained in the framework of the Regge model under these circumstances out to a $|t|$ value of approximately 2.3 $(GeV/c)^2$. The
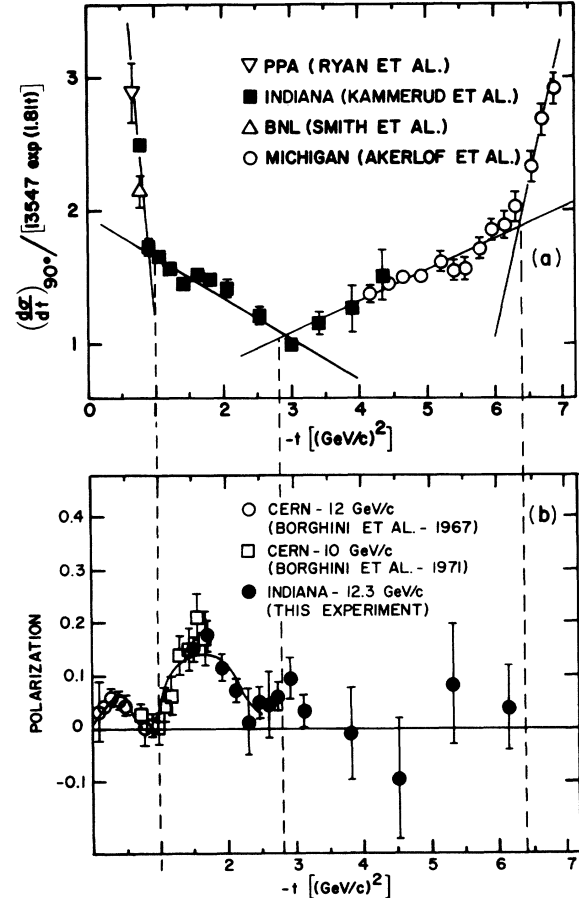

FIG. 3. (a) The differential cross sections in p-p elastic scattering at $\theta_{c.m.} = 90°$ normalized by an exponential in t to accentuate the details of the structure. The references for the data from other experiments are given in Ref. 8. $d\sigma/dt$ is measured in $\mu b/(GeV/c)^2$. (b) The p-p elastic polarization at 10.0 and 12.3 GeV/c and fits from the parton model proposed by Neal and Nielsen (Ref. 8).

predicted polarization beyond $|t| = 2.3$ (GeV/c)² is, however, vanishingly small for all reasonable amplitude parametrizations presently studied. Moreover, the Regge prediction for the energy dependence of the polarization at fixed t is found to be inconsistent with existing data.

The structure observed in the polarization can be easily accounted for in an optical model. In the optical model of Chu and Hendry[7] the nonflip amplitudes φ_1 and φ_3 are represented by smooth distributions in the impact parameter b for $b < R$ (where R is the effective proton radius), the single-flip amplitude φ_5 is assumed to receive its principal contributions from peripheral impact parameters near $b = R$, and φ_2 and φ_4 are neglected. The result is that the polarization is roughly proportional to $J_1^2(R\sqrt{-t})/\sqrt{-t}$. A fit to our data with this model is illustrated in Fig. 2 by the solid line. The amplitudes are also simultaneously constrained to fit the elastic differential cross section.

Neal and Nielsen[8] have studied certain conditions which are expected to be imposed on the p-p elastic polarization by the assumption of nucleon constituent structure. The various "regions" which appear in the fixed angle ($\theta_{c.m.} = 90°$) differential cross section are assumed to be due to n partons in one proton scattering from n partons in the other proton, where n changes in going from one region to the next. The region defined by $0 \leq |t| \leq 1.0$ (GeV/c)² in Fig. 3(a) is assumed to correspond to $n = 1$, the region $1 \leq |t| \leq 2.5$ (GeV/c)² to $n = 2$, etc. Next the assumption is made that any polarization acquired by a parton in the parton-parton scattering process is fully transmitted to the final-state proton formed with that parton.

If the parton polarization parameter is designated by $S(t)$, then the p-p elastic polarization at a four-momentum transfer squared t in region n is given in the model by

$$P(t) = nS(t/n^2). \tag{3}$$

Thus, if S is determined in region 1 the p-p polarization in other regions can be predicted by using Eq. (3). The result of this procedure is shown in Fig. 3(b), where a fit to the data in region 1 is used to generate a prediction for region 2. This picture provides a consistent description of the polarization in these first two regions. However, in the next region the existing data do not exhibit sufficiently large polarization values to be consistent with Eq. (3). This may be an indication that the third region actually does not begin near $|t| = 2.5$ (GeV/c)² but at a substantially larger $|t|$ value instead. In this case the slope change observed in the fixed-angle cross section near $|t| = 2.5$ (GeV/c)² must be attributed to a transition effect between the $0 \leq |t| < 1.0$ (GeV/c)² region and the $|t| > 6.0$ (GeV/c)² region. High-accuracy large-$|t|$ polarization measurements would be of great value in further testing the validity of these ideas.

*Work supported by the U. S. Energy Research and Development Adminstration under Contract No. AT (11-1)-2009, Task A, and by the Alfred P. Sloan Foundation.

†Alfred P. Sloan Foundation Fellow.

[1] G. W. Abshire, C. M. Ankenbrandt, R. R. Crittenden, D. B. Curtis, R. M. Heinz, K. Hinotani, H. A. Neal, H. R. Petri, and D. R. Rust, Indiana University Technical Report No. C00-2009-72 (unpublished).

[2] G. W. Abshire, C. M. Ankenbrandt, R. R. Crittenden, R. M. Heinz, K. Hinotani, S. I. Levy, H. A. Neal, and D. R. Rust, Phys. Rev. D 9, 555 (1974).

[3] G. W. Abshire, C. M. Ankenbrandt, R. R. Crittenden, R. M. Heinz, K. Hinotani, H. A. Neal, and D. R. Rust, Phys. Rev. Lett. 32, 1261 (1974).

[4] M. Borghini, L. Dick, J. C. Olivier, H. Aoi, D. Cronenberger, G. Gregoire, Z. Janout, K. Kuroda, A. Michalowicz, M. Poulet, D. Sillou, G. Bellettini, P. L. Braccini, T. Del Prete, L. Foà, P. Laurelli, G. Sanguinetti, and M. Valdata, Phys. Lett. 36B, 501 (1971); only data out to $|t| \approx 1.7$ (GeV/c)² are presented from this reference since at the higher $|t|$ values the errors become significantly larger than those of the present experiment.

[5] M. L. Goldberger, M. T. Grisaru, S. W. MacDowell, and D. W. Wong, Phys. Rev. 120, 2250 (1960).

[6] A. W. Hendry and G. W. Abshire, Phys. Rev. D 10, 3662 (1974).

[7] S.-Y. Chu and A. W. Hendry, Phys. Rev. D 6, 190 (1972); T. Y. Cheng, S.-Y. Chu, and A. W. Hendry, ibid. 7, 86 (1973).

[8] H. A. Neal and H. B. Nielsen, Phys. Lett. 51B, 79 (1974).